Non-negative Matrix Factorization of Dynamic Images in Nuclear Medicine

Jae Sung Lee, Daniel D. Lee, Seungjin Choi, Kwang Suk Park, and Dong Soo Lee

Abstract--**Recently suggested non-negative matrix factorization (NMF) seems to overcome fundamental limitations of factor analysis at least in theoretical aspect. NMF cost function uses Poisson statistics as a noise model, rather than the Gaussian statistics, and provides a simple learning rule, in contrast to the tricky optimization in factor analysis. To study the feasibility of NMF for the analysis of dynamic image sequences in nuclear medicine, NMF was applied to $H_2{}^{15}O$ dynamic myocardial PET images acquired from dog studies, and the results were compared with those obtained by conventional factor analysis method. Using NMF we could obtain basis images corresponding to major cardiac components. Their time-activity curves showed reasonable shapes that we have been familiar with. With the assumption of proper number of factors, NMF presented good results at least similar with those by factor analysis. Our results showed that NMF would be feasible for image segmentation and factor extraction from dynamic image sequences in nuclear medicine.**

I. Introduction

By means of dynamic positron emission tomography (PET) study, quantitative information on regional physiological processes is obtainable. Water labeled with ^{15}O is a favorable radiopharmaceutical for the measurement of myocardial blood flow (MBF) using dynamic PET scan, since it is metabolically inert and its first-pass extraction across myocardium is high enough [1]-[2].

Owing to these attractive and straightforward properties of $H_2{}^{15}O$ as a flow agent, the kinetics of $H_2{}^{15}O$ can be described by the simple single compartment model. In conjunction with appropriate correction parameters for partial volume and spillover effect due to the limited spatial resolution of PET image and cardiac motion, MBF can be estimated using this kinetic model and the radioactivity concentration time activity curve (TAC) in arterial blood and myocardium [1]-[4].

Manuscript received Nov 7, 2001. This work was supported in part by the Korean Ministry of Science and Technology, and in part by BK21 Human Life Sciences.

Jae Sung Lee and Dong Soo Lee are with the Departments of Nuclear Medicine, Seoul National University College of Medicine, Seoul 110-744, Korea (e-mail: jaes@snuvh.snu.ac.kr & dsl@plaza.snu.ac.kr).

Kwang Suk Park is with the Department of Biomedical Engineering, Seoul National University College of Medicine, Seoul 110-744, Korea (e-mail: kspark@snuvh.snu.ac.kr)

Daniel D. Lee is with the Bell Laboratories, Lucent Technologies, Murray Hill, New Jersey, USA (e-mail: ddlee@lucent.com).

Seungjin Choi is with the Department of Computer Science and Engineering, Pohang University of Science and Technology, Pohang, Korea (seungjin@postech.ac.kr).

The application of this kind of analysis to myocardial PET image is usually easier than other images since we can obtain the arterial input function from the left ventricular (LV) blood pool activity in the PET image without any sampling of arterial blood. The derivation of LV input function from myocardial $H_2{}^{15}O$ PET is, however, not so easy since $H_2{}^{15}O$ is rapidly diffused across the myocardium and distributed evenly over the ventricles and myocardium. The considerable amount of statistical noise generated in short dynamic frames as well as the diffusible property of $H_2{}^{15}O$ hinders the identification of the cardiac components required to define region of interest (ROI) on the LV region for input function and on the myocardium for tissue TAC.

A blood pool image, therefore, is often obtained by performing $C^{15}O$ PET scan, and the myocardium image is generated by subtracting a rescaled blood pool image from either a transmission image or an image of the washout phase of the dynamic $H_2{}^{15}O$ scan for ROI definition [2], [5]. However, several disadvantages have been reported with the use of the $C^{15}O$ scan: radiation dose to the patient, scan duration, and possibility of movement artifact due to misalignment between $C^{15}O$ and the other images increases, and additional gas delivery system and control are required [5].

Data driven approaches such as factor analysis [5]-[6] and independent component analysis [7] have been attempted to separate each cardiac component and to extract the LV input function from the dynamic $H_2{}^{15}O$ PET image itself. Since the pioneering works by Barber [8] and Di Paola *et al*. [9], factor analysis algorithm has been widely used for handling of dynamic image sequences in nuclear medicine [6], [10]. Although such a factor analysis method, based on principal component analysis followed by oblique rotation of factor loadings, has been considered a useful tool for processing dynamic images, factor analysis assumes Gaussian statistics, which may not be appropriate for gamma camera images. Also, the currently available methods for oblique rotation of factor loadings with assumptions of a priori knowledge are somewhat tricky to apply.

Recently suggested non-negative matrix factorization (NMF) seems to overcome this fundamental limitation of factor analysis at least in theoretical aspect [11]-[13]. One of the major advantages of NMF over factor analysis with positive constraints is that the NMF cost function uses Poisson statistics as a noise model. This is more appropriate

0-7803-7324-3/02/$17.00 © 2002 IEEE

for gamma camera images than the Gaussian model because the gamma camera images really represent some sort of photon counts. In addition, NMF provides a nice simple learning rule, which is guaranteed to converge monotonically without the need for setting any adjustable parameters such as a learning rate, in contrast to the tricky optimization in factor analysis.

To study the feasibility of NMF for the analysis of dynamic image sequences in nuclear medicine field, NMF was applied to $H_2{}^{15}O$ dynamic myocardial PET images, in which we intended to segment major cardiac components and derive their time-activity curves using NMF. The results were compared with those obtained by conventional factor analysis method.

II. Materials and Methods

A. Image Acquisition and Reconstruction

$H_2{}^{15}O$ PET scans were performed on seven dogs at rest (n=7) and after pharmacological stress (n=5) using adenosine or dipyridamole. All the scans were acquired with an ECAT EXACT 47 scanner (Siemens-CTI, Knoxville, TN), featuring an intrinsic resolution of 5.2 mm FWHM (full width at half maximum) and 47 simultaneous contiguous planar images of 3.4 mm thickness for a longitudinal field of view of 16.2 cm. Before $H_2{}^{15}O$ administration, transmission scanning was performed using three Ge-68 rod sources for attenuation correction. Dynamic emission scans (5sec×12, 10sec×9, 30sec×3) were initiated simultaneously with the injection of 555~740 MBq $H_2{}^{15}O$ and continued for four minutes.

Transaxial images were reconstructed, by means of a filtered back-projection algorithm employing a Shepp-Logan filter with cut-off frequency of 0.3 cycles/pixel, as 128×128×47 matrices with a size of 2.1×2.1×3.4 mm.

B. Preprocessing

The initial eighteen frames (two minutes) of PET images were used for analysis. The dynamic PET images were also reoriented to short axis and re-sampled to produce 1 cm thickness in order to increase the signal to noise ratio. We reoriented each frame of the dynamic images using the parameters for rotation and the translation determined upon static images, which were obtained by summing dynamic images.

Only the cardiac regions were then masked to remove the extra-cardiac components and to reduce the quantity of data and hence the burden of calculation. The mask size was 32×32 (pixel×pixel), and the masked images were resized to 8×8 images to reduce statistical fluctuation. The resulting masked images with dimensions of 8×8×6×18 (pixel×pixel×plane×frame) were reformatted to 18×384 (frame×pixel) matrices for further analysis.

C. Factor Analysis

We used the factor analysis algorithm originally established by Barber [8] and Di Paola *et al*. [9] and employed for extracting ventricular input functions and tissue curves from dynamic myocardial PET using $^{13}NH_3$ and FDG [10].

The underlying assumption behind factor analysis is that the observable time activity curve for each voxel in the PET images is equivalent to the weighted summation of the pure physiological factors, such as the right ventricular (RV), LV, and tissue time activity curves. Reformatted 384 TACs of the pixels (dixels) in the mask were normalized and submitted for the principal component analysis (PCA) to determine a low-dimensional subspace in which mainly the relevant part of the dixels is represented. Oblique rotation of the basis vectors from the PCA was performed to obtain non-orthogonal basis vectors, namely the factors, having a physical or physiological meaning. The iterative apex-seeking method suggested by Barber was used for oblique rotation [8]. Stating values for apex-seeking were selected by the method suggested by Di Paola *et al*. [9].

Factor images were then computed by means of the orthogonal projections of all the dixels of the original masked dynamic images (32×32×6×18 matrix) onto the factors [8], [9]. The number of factors was determined by visual assessment of the factors and factor images. Since factor analysis produced only the factors and factor images with unfamiliar shapes when the assumed number of factors was incorrect, the determination of the number of factors by visual assessment was easy and reliable.

Since each factor was in normalized units, LV input function was obtained by rescaling the factor corresponding to the LV TAC as performed by Wu and her colleagues in their factor analysis for $^{13}NH_3$ and FDG PET data [10]. We used the average of the pixel values above 50 % of the maximum pixel value in the LV factor image as a scale factor.

D. Non-negative Matrix Factorization

We followed notations used by Lee and Seung originally [11]-[13]. Let's assume a dynamic image with n non-negative voxels and m frames, and reformat the image as an $n \times m$ matrix V, each column of which correspond to each frame of dynamic image. NMF factorize this matrix V into an $n \times r$ matrix W and an $r \times m$ matrix H approximately ($V \approx WH$) with a constraint that negative elements are not allowed in W and H. This NMF factorization is optimized by minimizing the cost function to measure the distance between V and WH, in which each voxel $V_{i\mu}$is regarded as a summation of the product $(WH)_{i\mu}$ and Poisson noise. Consequently, the μth column of W (μ= 1, 2, ···, r) represents the μth basis image, and the μth row of H corresponds to the time-activity curve of this basis image.

Two alternative formulation of NMF can be used differently according to the cost function to be minimized. In this study, we used a following update rule that makes the divergence between V and WH minimized with the non-negativity constraints, rather than Euclidean distance between V and WH [12].

$$W_{ia} \leftarrow W_{ia} \sum_{\mu} \frac{V_{i\mu}}{(WH)_{i\mu}} H_{a\mu}, \quad W_{ia} \leftarrow \frac{W_{ia}}{\sum_{j} W_{ja}}$$

$$H_{a\mu} \leftarrow H_{a\mu} \sum_{i} W_{ia} \frac{V_{i\mu}}{(WH)_{i\mu}}$$

Each frame of the masked region was then submitted to the NMF. All the data points were passed 100 times into the network iteratively. The average of the voxel values above 50 % of maximum voxel value in each basis image was used to rescale its time-activity curve.

III. Results

Fig.2 shows the basis images (left) and their time-activity curves (right) obtained using NMF from a dog PET data at rest. It is evident that the three basis images correspond to major three cardiac componenents, a) right ventricle, b) left venticle, c) myocardium. Also, their time-activity curves showed reasonable shapes that we were familiar with (higher peak in right ventricle, more dispersion in left ventricle, and others).

With the assumption of proper number of factors, NMF presented good results at least similar with those by factor analysis. Although further verification is necessary, our preliminary study shows that NMF would be feasible for image segmentation and factor extraction from dynamic image sequences in nuclear medicine.

IV. References

[1] S. R. Bergmann, K. A. A. Fox, A. L. Rand, K. D. McElvany, M. J. Welch, J. Markham and B. E. Sobel, "Quantification of regional myocardial blood flow in vivo with $H_2{}^{15}O$," *Circulation*, vol. 70, pp. 724-733, 1984.

[2] L. I. Araujo, A. A. Lammertsma, C. G. Rhodes, E. O. McFalls, H. Iida, E. Rechavia, A. Galassi, R. De Silva, T. Jones and A. Maseri, "Noninvasive quantification of regional myocardial blood flow in coronary artery disease with oxygen-15-labeled carbon dioxide inhalation and positron emission tomography," *Circulation*, vol. 83, pp. 875-885. 1991.

[3] P. Herrero, J. Markham, D. W. Myears, C. J. Weiheimer and S. R. Bergmann, "Measurement of myocardial blood flow with positron emission tomography: correction for count spillover and partial volume effects," *Math. Comput. Model*, vol. 11, pp. 807-812, 1988.

[4] H. Iida, Y. Tamura, K. Kitamura, P. M. Bloomfield, S. Eberl and Y. Ono, "Histochemical correlates of ^{15}O-water-perfusible tissue fraction in experimental canine studies with old myocardial infarction", *J. Nucl. Med.*, vol. 41, pp. 1737-1745, 2000.

[5] F. Hermansen, J. Ashburner, T. J. Spinks, J. S. Kooner, P. G. Camici and A. A. Lammertsma, "Generation of myocardial factor images directly from the dynamic oxygen-15-water scan without use of an oxygen-15-carbon monoxide blood-pool scan," *J. Nucl. Med.*, vol. 39, pp. 1696-1702, 1998.

[6] J. Y. Ahn, D. S. Lee, J. S. Lee, S-K. Kim, G. J. Cheon, J. S. Yeo, S-A. Shin, J-K. Chung, M. C. Lee, "Quantification of regional myocardial blood flow using dynamic $H_2{}^{15}O$ PET and factor analysis", *J. Nucl. Med.*, vol. 42, no. 5, pp. 782-787, 2001

[7] J. S. Lee, D. S. Lee, J. Y. Ahn, G. J. Cheon, S-K. Kim, J. S. Yeo, K. S. Park, J-K. Chung, M. C. Lee, "Blind separation of cardiac components and extraction of input function from $H_2{}^{15}O$ dynamic myocardial PET using independent component analysis", *J. Nucl. Med.*, vol. 42, no. 6, pp. 938-943, 2001.

[8] D. C. Barber, "The use of principal components in the quantitative analysis of gamma camera dynamic studies," *Phys. Med. Biol.*, vol. 25, pp. 283-292, 1980.

[9] R. Di Paola, J. P. Bazin, F. Aubry, A. Aurengo, F. Cavailloles, J. Y. Herry and E. Kahn, "Handling of dynamic sequences in nuclear medicine," *IEEE Trans. Nucl. Sci.*, vol. NS29, pp. 1310-1321, 1982.

[10] H-M. Wu, C. K. Hoh, Y. Choi, H. R. Schelbert, R. A. Hawkins, M. E. Phelps and S. C. Huang, "Factor analysis for extraction of blood time-activity curves in dynamic FDG-PET studies," *J. Nucl. Med.*, vol. 36, pp. 1714-1722, 1995.

[11] D. D. Lee, H. S. Seung, "Unsupervised learning by convex and conic coding", *Adv. Neural Info. Proc. Syst.*, vol. 9, pp. 515–521, 1997.

[12] D. D. Lee, H. S. Seung, "Learning the parts of objects by non-negative matrix factorization", *Nature*, vol. 401, pp. 788-791, 1999.

[13] D. D. Lee, H. S. Seung, "Algorithms for non-negative matrix factorization", *Adv. Neural Info. Proc. Syst.*, vol. 13, 2001.

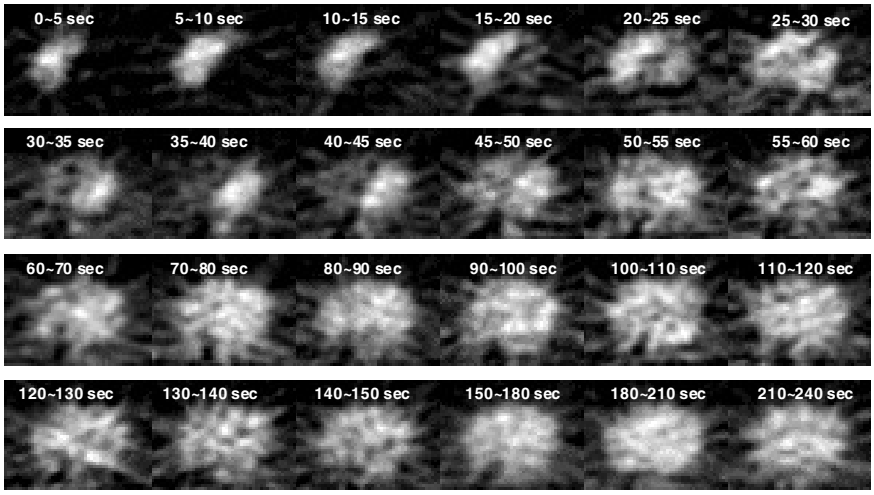

Fig. 1. $H_2{}^{15}O$ dynamic myocardial PET (normalized count in each frame).

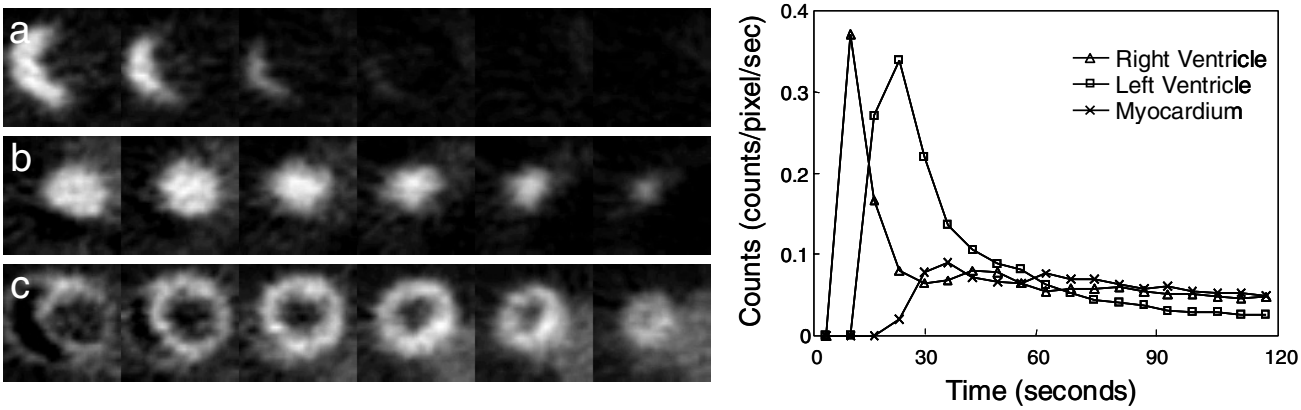

Fig. 2. Basis images (left) and their time-activity curves (right) obtained using NMF from a dog PET data at rest.